$\langle s^2 \rangle \mu^2$ is near 100. This type of behavior is not evident in either Figure 1 or Figure 2. However, we must point that μ^{-1} must approach the length of a C–C bond if $\langle s_{ij}^2 \rangle \mu^2$ is to be near 100 for the subchains considered here. Therefore somewhat different behavior might be observed with much longer subchains.

Acknowledgment is made to the donors of the Petroleum Research Fund, administered by the American Chemical Society, for support of this research.

References and Notes

(1) Flory, P. J. *Macromolecules* **1974**, *7*, 381.
(2) Mattice, W. L.; Santiago, G. *Macromolecules* **1980**, *13*, 1560.
(3) Mattice, W. L. *Macromolecules* **1981**, *14*, 1485.
(4) Mattice, W. L. *Macromolecules* **1981**, *14*, 1491.
(5) Kranbuehl, D. E.; Verdier, P. H. *J. Chem. Phys.* **1977**, *67*, 361.
(6) Mazur, J.; Guttman, D. M.; McCrackin, F. L. *Macromolecules* **1973**, *6*, 872.
(7) Gobush, W.; Šolc, K.; Stockmayer, W. H. *J. Chem. Phys.* **1974**, *60*, 12.
(8) Abe, A.; Jernigan, R. L.; Flory, P. J. *J. Am. Chem. Soc.* **1966**, *88*, 631.
(9) Debye, P. *Ann. Phys. (Leipzig)* **1915**, *46*, 809.
(10) Debye, P. *J. Phys. Chem.* **1947**, *51*, 18.
(11) Yoon, D. Y.; Flory, P. J. *Macromolecules* **1976**, *9*, 294.
(12) Zierenberg, B.; Carpenter, D. K.; Hsieh, J. H. *J. Polym. Sci., Polym. Symp.* **1976**, *No. 54*, 145.
(13) McIntyre, D.; Mazur, J.; Wims, A. M. *J. Chem. Phys.* **1968**, *49*, 2887.
(14) Mazur, J.; McIntyre, D.; Wims, A. M. *J. Chem. Phys.* **1968**, *49*, 2896.
(15) Mijnlieff, P. F.; Coumou, D. J.; Meisner, J. *J. Chem. Phys.* **1970**, *53*, 1775.
(16) Ohta, T.; Oono, Y.; Freed, K. F. *Macromolecules* **1981**, *14*, 1588.

Small-Angle Neutron Scattering from Elastomeric Networks. Junction Fluctuations and Network Unfolding

Robert Ullman

Research Staff, Ford Motor Company, Dearborn, Michigan 48121. *Received July 29, 1981*

ABSTRACT: Theoretical calculations of small-angle neutron scattering (SANS) from labeled chains in polymeric networks are presented. These start from the phantom network as a point of departure and include two additional properties of real networks absent in the phantom model. First of all, the reduction of fluctuations of cross-link junctions by network entanglements is introduced according to a model pioneered by Flory. Secondly, a concept of network unfolding without chain deformation is introduced. SANS experiments on deformed networks provide support for the thesis that, in some cases, chain deformation is less than that calculated from the phantom network model. This becomes particularly striking if the model is modified to take into account reduced junction fluctuations.

Introduction

The unique elasticity of rubber polymeric networks arises from the flexibility of the macromolecules of which the network is composed. A statistical thermodynamic theory of these networks, formulated by James[1] and James and Guth[2] and modernized and extended by Graessley,[3,4] Ronca and Allegra,[5] Deam and Edwards,[6] and Flory,[7] is known as the phantom network model. This is an apt name since it emphasizes the hypothetical ability of chains to pass through one another, a property which makes calculations tractable but which is regrettably one of the serious weaknesses of the theory.

There have been a number of indications that the phantom network model is not in accord with experiment. The experiments of Lloyd and Alfrey[8,9] on cross-linked networks prepared under different conditions are not consistent with the phantom model. Pearson and Graessley[10] find that stresses in ethylene–propylene copolymer networks exceed predictions derived for a phantom network. They regard the excess stress as an additional contribution from entanglements. By contrast, Mark and Sullivan[11] find no such discrepancies in their investigation of cross-linked poly(dimethylsiloxane) rubber. Ferry and colloborators[12] conducted a series of studies on polybutadiene networks prepared by cross-linking oriented polymer molecules. The interpretation of these experiments requires the assignment of stress, in large part, to an entanglement network.

Small-angle neutron scattering (SANS) is used to measure the size and shape of deuterium-labeled polymer molecules in an ordinary hydrogenous polymer matrix[13,14] and has been applied to networks[15-17] in a few cases. Benoit et al. have done this with cross-linked polystyrene gels[18] and have found, in some cases, that swelling is less than that given by the phantom network model. An investigation of osmotically deswollen polystyrene networks by Bastide et al.[19] has shown that chain deformation in partially swollen materials changes very little with degree of swelling. Early experiments by Hinkley et al.[20] and Clough et al.[21] show chain deformation consistent with the phantom network, but later experiments by Beltzung et al.[22] on siloxane networks yield results which vary over a range and in which the network with the highest molecular weight between cross-links deforms less than the phantom network. Han, in a SANS investigation of a trifunctional polyisoprene network,[23] has found, depending on the sample, deformation both greater and less than that predicted by the phantom network model.

Flory[24] and Erman and Flory[25] have proposed modifications of the phantom network model in which junction fluctuations are partially suppressed. Flory, referring to previous experiments,[26,27] finds that the suppression of junction fluctuations is considerable.[28] The effect of reducing fluctuations is to predict that chain deformation is greater than that given by the phantom model. This is found in some cases, but the reduction in junction fluctuations cannot account for chain deformations less than that expected from a phantom network.

Network Unfolding without Chain Deformation

Consider the following three explanations for network deformations which are less than would be found in a phantom network.

1. The measurement of dimensions by SANS is inaccurate and unreliable.

2. The preparation of networks is imperfect, dangling chain ends exist, and these lead to lower chain extensions upon deformation than for a perfect network.

0024-9297/82/2215-0582$01.25/0

3. Chain deformation need not be affine and in certain circumstances is less than affine.

The prudent investigator is aware that SANS measurements can be systematically in error and also that it is easy to incorporate network defects which lead to average chain deformations less than anticipated. Nevertheless, the evidence, in the judgment of this observer, seems to require an essential modification of the theory.

Consider the possibility that the vectors connecting chain ends deform less than that predicted by the affine hypothesis. To illustrate this, a hypothetical network designed to contain no trapped entanglements, and therefore unrealistic, is chosen as a model. The network is formed on a regular lattice with each chain cross-linked with its end segments on neighboring lattice points. The collapsed network has a normal density, the molecular weight between cross-links is of the order of 10 000, and the root-mean-square end-to-end distance is that of an unperturbed random flight Gaussian coil. The junction points which are near geometric neighbors are mostly remote in chain space, and topologically neighboring junctions (those connected directly by a single network chain) are only rarely nearest geometric neighbors.

If the hypothetical network conformed to the phantom model, the elastic free energy of swelling in a solvent would be $(3kT/2)\nu(1 - 2/f)(\lambda^2 - 1)$, where ν is the number of elastically effective chains, f, the network functionality, and λ, the linear macroscopic expansion of the sample. In this view λ is also the ratio of the mean distance between each pair of chain ends after swelling to that before swelling. With network unfolding and junction rearrangement, chains will extend less than the macroscopic expansion. The driving force for the rearrangement is a reduction in elastic free energy. A similar argument applies for uniaxial stretching and other types of elastic deformation.

Real networks are entangled. Entanglements drastically inhibit network unfolding, and since the extent of entanglement is intimately linked to the materials and procedures in network preparation, the degree to which networks unfold with reduced chain deformation will vary from one system to another. It is to be anticipated that cross-linking in solution will lead to fewer entanglements than cross-linking in bulk, and therefore, other things being equal, network unfolding will be of greater importance in networks prepared at higher dilution. Chains in a network formed in solution repel each other when the solvent is removed. Therefore, the idealized network described above may not be able to collapse to a density of a normal bulk material. The example is only intended to illustrate network unfolding, which can take place in any system where the number of trapped entanglements are few.

Junction points can be divided in two classes, topological neighbors which are connected by a polymer chain and topologically remote pairs which are not. A further classification of topologically remote junctions is possible but is not germane to the present discussion. Most geometric near neighbors will be topologically remote if the cross-link density is not too high. Upon deformation by either swelling or stretching, distances between topological neighbors may change less than in a phantom network, a distortion compensated by rearrangement of topologically remote junction pairs. This must take place in such a way that the overall distribution of junction points remains homogeneous.

In the Alfrey–Lloyd papers,[8,9] it is shown that networks prepared at higher dilution swell to a greater extent. This can be understood as a consequence of the disentanglement of a network which is folded and contains relatively few trapped entanglements.

In the phantom network, the x component of the mean end-to-end distance of a typical chain averaged over all chains deforms according to

$$\langle \bar{X}^2 \rangle = \lambda_x^2 \langle (\bar{X}^0)^2 \rangle \tag{1}$$

where λ_x is the x component of the macroscopic deformation of the rubber. The bar symbolizes a time average for a single chain and the angular brackets denote an ensemble average over all chains. In a nonaffine model there is a microscopic deformation at the level of the end-to-end distance given by

$$\langle \bar{X}^2 \rangle = \lambda_x^{*2} \langle (\bar{X}^0)^2 \rangle \tag{2a}$$

where

$$\lambda_x^{*2} = (1 - \alpha)\lambda_x^2 + \alpha \tag{2b}$$

Affine deformation of $\bar{X}$ corresponds to $\alpha = 0$, while at $\alpha = 1$, there is no chain deformation as the macroscopic sample is deformed. The extreme case of the idealized unentangled network discussed above leads to the limit $\alpha = 1$ for extensions which are not too great. It is also evident that the form of eq 2b is arbitrary save for the fact that it has proper limiting values. The arbitrary form does not restrict its generality, however; any other formal equation which behaved properly at the limits and changed monotonically with ease of disentanglement would be equally satisfactory.

Neutron Scattering of Gaussian Networks

A polymeric network containing a small percentage of deuterium-labeled chains scatters neutrons in excess of that of the unlabeled material. The excess scattering is proportional to molecular weight of the labeled chains, M, to their concentration, c, to a contrast factor, $(\Delta b)^2$, and to a form factor, $S(\mathbf{q})$.

$$I(\mathbf{q}) = KMc(\Delta b)^2 S(\mathbf{q}) \tag{3}$$

$\mathbf{q}$ is the wave vector, equal to $2\pi/\lambda'$ multiplied by the difference in unit vectors taken in the direction of incident and scattered beams. The magnitude of $\mathbf{q}$, designated as q, equals $(4\pi/\lambda') \sin(\theta/2)$, λ' being the neutron wavelength and θ the scattering angle. K is a constant which contains machine parameters and neutron flux. The term of interest for determination of chain shape and size is $S(\mathbf{q})$, which is given by

$$S(\mathbf{q}) = \frac{1}{N^2} \sum_{i,j=1}^{N} e^{i\mathbf{q}\cdot\mathbf{r}_{ij}} \tag{4}$$

$\mathbf{r}_{ij}$ is the vector connecting the ith and jth segment of a single labeled chain. There are N segments on each polymer chain. For Gaussian chains centered at $\mathbf{r}_{ij} = 0$ and in which $\mathbf{r}_{ij}$ depends on $|i - j|$ and not i and j separately, $S(\mathbf{q})$ may be written in the form of a single integral

$$S(\mathbf{q}) = 2\int_0^1 (1 - w) \exp[-x(w + bw^2)]\, dw \tag{5}$$

x equals $q^2(R_g^0)^2/6$, where R_g^0 is the radius of gyration of the free polymer chain in the absence of constraints in the unperturbed state. Equation 5 is easily reduced to elementary functions and error functions ($b > 0$) or Dawson's integral ($b < 0$). The steps leading from eq 4 to eq 5 are presented in earlier publications.[15,17] See Appendix. Briefly, by letting $w = |i - j|/N$ and replacing the sums by an integral, eq 4 becomes

$$S(\mathbf{q}) = 2\int_0^1 (1 - w) \exp[i\mathbf{q}\cdot\mathbf{r}_{ij}] W(\mathbf{r}_{ij})\, d\mathbf{r}_{ij}\, dw \tag{6a}$$

$$W(\mathbf{r}_{ij}) = (3/2\pi\langle r_{ij}^2\rangle)^{3/2} \exp[-3r_{ij}^2/2\langle r_{ij}^2\rangle] \quad (6b)$$

Equations 6a and 6b are dealt with most simply by converting to Cartesian coordinates. One finds

$$S(\mathbf{q}) = 2\int_0^1 (1-w) \exp[-(q_x^2\langle x_{ij}^2\rangle - q_y^2\langle y_{ij}^2\rangle - q_z^2\langle z_{ij}^2\rangle)/2]\, dw \quad (7)$$

In the free Gaussian chain one has $\langle x_{ij}^2\rangle = \langle y_{ij}^2\rangle = \langle z_{ij}^2\rangle = (Nb^2/3)w$. If the end points of the Gaussian chain are constrained so that the mean-square end-to-end distance is R^2 ($R = (X,Y,Z)$), one finds

$$\langle z_{ij}^2\rangle = (Nb^2/3)(w - w^2) + w^2\langle Z^2\rangle \quad (8)$$

Similar equations apply for $\langle x_{ij}^2\rangle$ and $\langle y_{ij}^2\rangle$. To simplify the calculation, the scattering system is fixed in a geometry in which the neutron beam is in the X direction and the detector lies in the YZ plane. If the scattering angles are small, $\mathbf{q}$ also lies in the YZ plane, $q_x \approx 0$, $q_y = q \sin\phi$, and $q_z = q\cos\phi$, where ϕ is the azimuthal angle in the YZ plane measured with respect to the Z axis. Equation 7 becomes

$$S(\mathbf{q}) = 2\int_0^1 (1-w) \exp[-x(w - w^2 + w^2F(Y,Z,\phi))]\, dw \quad (9a)$$

$$F(Y,Z,\phi) = (\langle Z^2\rangle/\langle (Z^0)^2\rangle)\cos^2\phi + (\langle Y^2\rangle/\langle (Y^0)^2\rangle)\sin^2\phi \quad (9b)$$

The correspondence of eq 9a and eq 5 is evident. The calculation of $\langle Z^2\rangle/\langle (Z^0)^2\rangle$ and $\langle Y^2\rangle/\langle (Y^0)^2\rangle$ is carried out following the method designed for the phantom network, but using λ^*, the molecular stretching factor, rather than the macroscopic deformation. Thus

$$\langle \bar{Z}^2\rangle = \lambda_z^{*2}\langle (\bar{Z}^0)^2\rangle \quad (10a)$$

$$Z = \bar{Z} + \delta Z \quad (10b)$$

$$\langle Z^2\rangle = \langle \bar{Z}^2\rangle + \langle (\delta Z)^2\rangle \quad (10c)$$

δZ is the fluctuation in Z, eq 10c is a consequence of the independence of Z and δZ ($\langle Z\,\delta Z\rangle = 0$). In a phantom network, $\langle (\delta Z)^2\rangle = (2/f)\langle (Z^0)^2\rangle$. Since eq 10c is valid in both the undeformed and stretched (or swollen) states, the phantom network result (modified to use molecular stretching factors) becomes

$$\langle (\bar{Z}^0)^2\rangle = \left(\frac{f-2}{f}\right)\langle (Z^0)^2\rangle \quad (11a)$$

$$\langle \bar{Z}^2\rangle = \lambda_z^{*2}\left(\frac{f-2}{f}\right)\langle (Z^0)^2\rangle \quad (11b)$$

$$\langle Z^2\rangle = \left(\lambda_z^{*2}\left(\frac{f-2}{f}\right) + \frac{2}{f}\right)\langle (Z^0)^2\rangle \quad (11c)$$

A similar argument is used when junction fluctuations are inhibited by entanglements. In this case $\langle \delta Z^2\rangle$ is decreased and, according to the Flory hypothesis,[24] is anisotropic. The Flory argument used here is modified to deal with fluctuations of distances between chain ends rather than fluctuations of positions.

The fluctuation in the mean-square end-to-end distance of a chain in the network is reduced by entanglements to

$$\langle (\delta Z)^2\rangle = \frac{2}{f(1 + \kappa\lambda_z^{*-2})}\langle (Z^0)^2\rangle \quad (12)$$

The phantom network result is found by setting α and κ to zero. As κ approaches infinity, fluctuations of the junction points vanish. The contribution of the entanglements to the junction fluctuations is affine in the molecular deformation, λ^*. Using eq 10a and 10c for the undeformed network, we find

$$\langle (\bar{Z}^0)^2\rangle = \left(1 - \frac{2}{f(1+\kappa)}\right)\langle (Z^0)^2\rangle \quad (13a)$$

$$\langle \bar{Z}^2\rangle = \lambda_z^{*2}\left(1 - \frac{2}{f(1+\kappa)}\right)\langle (Z^0)^2\rangle \quad (13b)$$

$$\langle Z^2\rangle = \left(\lambda_z^{*2}\left(1 - \frac{2}{f(1+\kappa)}\right) + \frac{2}{f(1+\kappa\lambda_z^{*-2})}\right)\langle (Z^0)^2\rangle \quad (13c)$$

Equations 7, 9, and 13c completely determine $S(\mathbf{q})$.

In a uniaxially stretched sample which does not change its volume upon elongation, $\lambda_z^* = \lambda^*$, and $\lambda_x^* = \lambda_y^* = \lambda^{*-1/2}$.

The constant b of eq 5 is, in this case,

$$b = \lambda^{*2}\left[\left(1 - \frac{2}{f(1+\kappa)}\right) + \frac{2}{f(1+\kappa\lambda^{*-2})}\right]\cos^2\phi + \left[\frac{1}{\lambda^*}\left(1 - \frac{2}{f(1+\kappa)}\right) + \frac{2}{f(1+\kappa\lambda^*)}\right]\sin^2\phi - 1 \quad (14)$$

In a stretched sample, the scattering is usually measured parallel and perpendicular to the direction of stretch. $S_\parallel(\mathbf{q})$ is obtained from eq 14 by setting $\phi = 0$; $S_\perp(\mathbf{q})$ results from $\phi = 90°$.

Turning to the problem of isotropic swelling of a network, $\lambda_x^* = \lambda_y^* = \lambda_z^* = \lambda^*$. In this situation

$$b = \lambda^{*2}\left(1 - \frac{2}{f(1+\kappa)}\right) + \frac{2}{f(1+\kappa\lambda^{*-2})} - 1 \quad (15)$$

The radius of gyration is obtained from $S(\mathbf{q})$ from the formula

$$S(\mathbf{q}) = 1 - q^2R_g^2/3 + \mathcal{O}(q^4) \quad (16a)$$

for an isotropic scatterer. This result does not apply for an oriented material. The radii $R_\parallel^2$ and $R_\perp^2$ are defined by

$$S_\parallel(\mathbf{q}) = 1 - q^2R_\parallel^2/3 + \mathcal{O}(q^4) \quad (16b)$$

$$S_\perp(\mathbf{q}) = 1 - q^2R_\perp^2/3 + \mathcal{O}(q^4) \quad (16c)$$

and R_g^2 is given by

$$R_g^2 = (R_\parallel^2 + 2R_\perp^2)/3 \quad (16d)$$

In a uniaxially oriented network

$$R_\parallel^2 = (Nb^2/12)\left[1 + \lambda^{*2}\left(1 - \frac{2}{f(1+\kappa)}\right) + \frac{2}{f(1+\kappa\lambda^{*-2})}\right] \quad (17a)$$

$$R_\perp^2 = (Nb^2/12)\left[1 + \lambda^{*-1}\left(1 - \frac{2}{f(1+\kappa)}\right) + \frac{2}{f(1+\kappa\lambda^*)}\right] \quad (17b)$$

R_g^2 in an isotropic swollen network is given by

$$R_g^2 = (Nb^2/12)\left[1 + \lambda^{*2}\left(1 - \frac{2}{f(1+\kappa)}\right) + \frac{2}{f(1+\kappa\lambda^{*-2})}\right] \quad (17c)$$

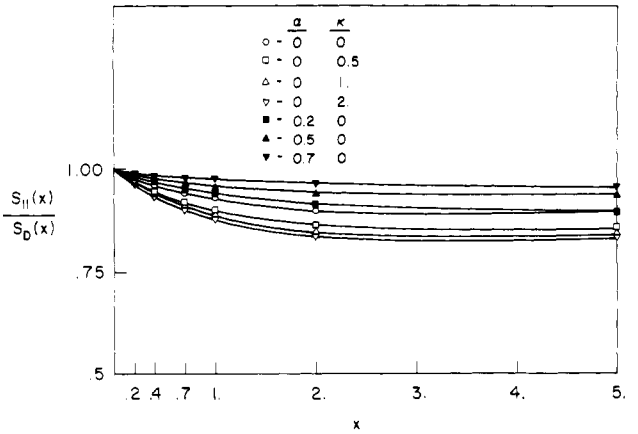

Figure 1. $S_{\parallel}(x)/S_D(x)$ vs. x for a uniaxially stretched rubber. The network is tetrafunctional, $\lambda = 1.5$. This figure also applies to $S(x)/S_D(x)$ for a swollen rubber.

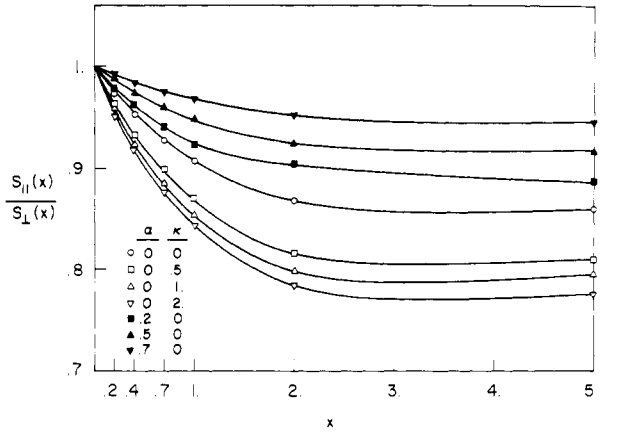

Figure 2. $S_{\parallel}(x)/S_{\perp}(x)$ vs. x for a uniaxially stretched rubber. The network is tetrafunctional, $\lambda = 1.5$.

Note that the formulas for $R_{\parallel}^2$ of eq 17a and R_g^2 of eq 17c are identical. However, λ^* has a different meaning in the two cases. A similar correspondence holds between $S_{\parallel}(\mathbf{q})$ of a polymer chain in a simply stretched rubber and $S(\mathbf{q})$ for an isotropic system. The identical forms are very useful in easing the tedium of numerical calculations.

The scattering intensity at an azimuthal angle ϕ, $S_{\phi}(\mathbf{q})$, is not obtainable by superimposing $S_{\parallel}(\mathbf{q})$ and $S_{\perp}(\mathbf{q})$ but must be obtained directly by substituting eq 14 in eq 5.

In the following section, some numerical results are presented in graphs and tables. These demonstrate how SANS results for a network with constraints on junction fluctuations (κ) and network unfolding (α) differ from that calculated for the idealized phantom model.

Numerical Results

The numerical examples are limited in number and are intended as illustrations. A few results for $S(\mathbf{q})$ and R_g^2 are presented for isotropically swollen networks, as well as for $S_{\parallel}(\mathbf{q})$ and $S_{\perp}(\mathbf{q})$ and $R_{\parallel}^2$ and $R_{\perp}^2$ for uniaxially stretched networks. The q dependence of the scattering is contained in the reduced variable $x = q^2(R_g^0)^2$ and therefore $S(\mathbf{q})$ will be referred to as $S(x)$ in the figures. Other parameters of the system, the macroscopic distortion λ, the network functionality f, the angle of observation ϕ, the junction fluctuation parameter κ, and the network unfolding parameter α, all appear as part of the lumped constant b.

Consider first the scattering function of a uniaxially deformed tetrafunctional network. In Figure 1, the calculation is performed for a chain in a network stretched to 150% of its initial length. The plots show the ratio of the scattering function of a chain in the network measured parallel to the stretching direction, relative to the scattering of the free unperturbed molecule. The scattering function for the free Gaussian molecule was calculated by Debye[30] and takes the simple form $S_D(x) = 2(x - 1 + e^{-x})/x^2$. The curve for the phantom network is given by $\alpha = \kappa = 0$.

As κ increases, the decrease of $S(x)$ with x becomes more rapid, which signifies that molecular deformation is greater if junction fluctuations are inhibited. As α increases, the change in macroscopic dimensions is compensated in part by network unfolding, and chain deformation is less than that of the phantom network. Figure 2 shows the comparison of the scattering function taken parallel and perpendicular to the stretching direction of the same systems treated in Figure 1, plotted as $S_{\parallel}(x)/S_{\perp}(x)$ vs. x. Increasing κ increases the anisotropy and increasing α decreases the anisotropy. Figures 3 and 4 contain plots of $S_{\parallel}(x)/S_D(x)$ vs. x and $S_{\parallel}(x)/S_{\perp}(x)$ vs. x for the same network considered in Figures 1 and 2 except that the extension ratio is 3.0 rather than 1.5. Qualitatively, the effects are the same, but the magnitude of the anisotropy is greater as expected.

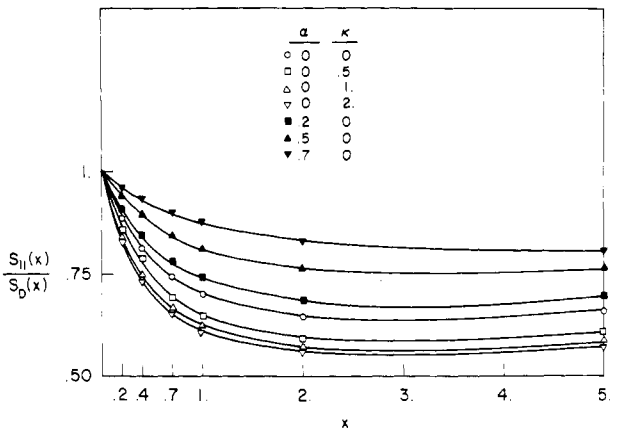

Figure 3. $S_{\parallel}(x)/S_D(x)$ vs. x for a uniaxially stretched rubber. The network is tetrafunctional, $\lambda = 3.0$. This figure also applies to $S(x)/S_D(x)$ for a swollen rubber.

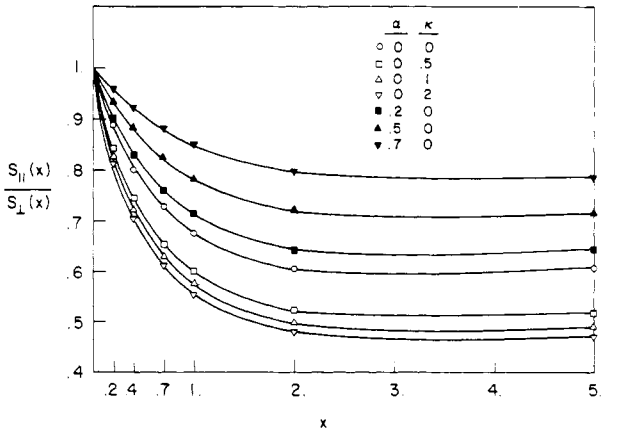

Figure 4. $S_{\parallel}(x)/S_{\perp}(x)$ vs. x for a uniaxially stretched rubber. The network is tetrafunctional, $\lambda = 3.0$.

It is clear that if both network unfolding and inhibition of junction fluctuations were considerable in the same network, one could obtain, by accidental compensation, scattering curves which differ very little from that of the phantom network. This is verified in some calculated results shown in Table I for a tetrafunctional network which is stretched 100%. One can hardly distinguish the calculated results of a phantom network from that of a real network with $\alpha = 0.5$ and $\kappa = 4$.

The relative importance of network unfolding and repression of junction fluctuations is resolvable by studying

Table I
Comparison of $S_{\parallel}(x)$ and $S_{\perp}(x)$ of a Phantom Network with a Real Network in Which Changes in α and κ Are Compensating[a]

x	$S_{\parallel}(x)$ $\alpha = \kappa = 0$	$S_{\parallel}(x)$ $\alpha = 0.5$, $\kappa = 4$	$S_{\perp}(x)$ $\alpha = \kappa = 0$	$S_{\perp}(x)$ $\alpha = 0.5$, $\kappa = 4$
0.2	0.8946	0.8962	0.9440	0.9474
0.4	0.8083	0.8107	0.8924	0.8986
0.7	0.7052	0.7084	0.8224	0.8318
1	0.6254	0.6287	0.7602	0.7719
2	0.4556	0.4586	0.5972	0.6122
5	0.2572	0.2588	0.3404	0.3513
10	0.1527	0.1534	0.1879	0.1923

[a] $\lambda = 2, f = 4$.

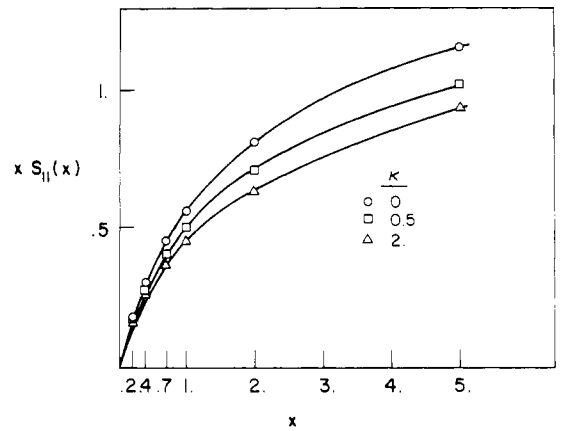

Figure 5. $xS_{\parallel}(x)$ vs. x for a uniaxially stretched rubber. The network is trifunctional, $\lambda = 3.0$, $\alpha = 0$. This figure also applies to $xS(x)$ for a swollen rubber.

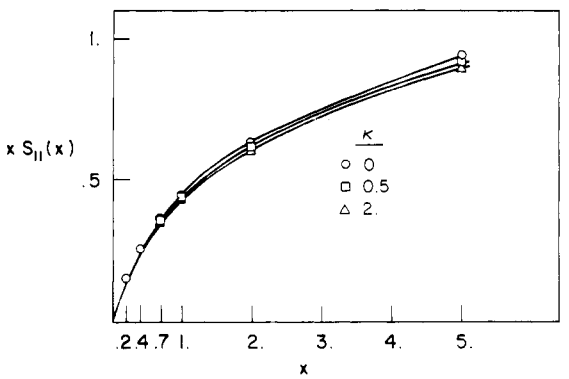

Figure 6. $xS_{\parallel}(x)$ vs. x for a uniaxially stretched rubber. The network is decafunctional, $\lambda = 3.0$, $\alpha = 0$. This figure also applies to $xS(x)$ for a swollen rubber.

networks of different functionality. The reason for this is that the cross-link junctions of networks of higher functionality are largely immobilized with or without entanglements, and changes in κ have minor influence only in modifying chain dimensions. This is easily shown by comparing the plots of $xS_{\parallel}(x)$ vs. x in Figure 5 with those of Figure 6. In Figure 5, the network is trifunctional, and constraints on junction fluctuations produce large changes in the scattering intensity. In Figure 6, the network is decafunctional, and changing κ has only a slight influence on scattering intensity.

Figures 7–12 contain plots of chain dimensions $R_{\parallel}^2$ and $R_{\perp}^2$ in networks of functionality 3, 4, and 10 as functions of λ, the macroscopic distortion of the network. In each figure the result for the phantom network is shown together with the changes in real networks in terms of κ and α. In all cases, the appropriate radii are calculated relative

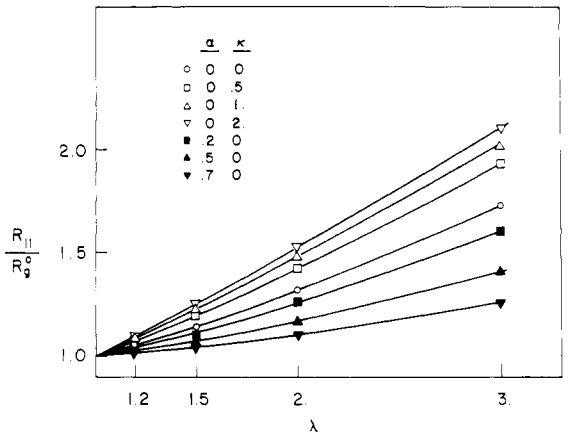

Figure 7. $R_{\parallel}/R_g^0$ vs. λ for a uniaxially stretched rubber. The network is trifunctional. This figure also applies to R_g/R_g^0 for a swollen rubber.

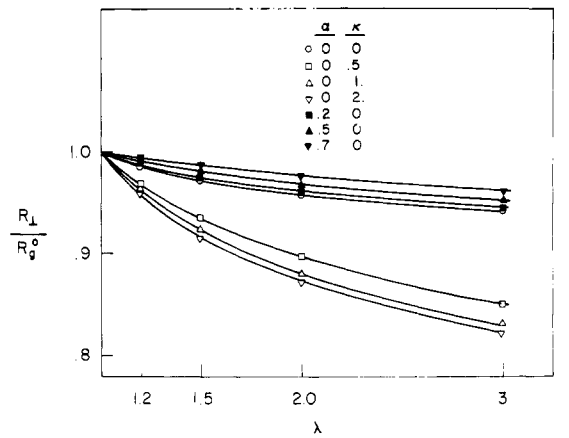

Figure 8. $R_{\perp}/R_g^0$ vs. λ for a uniaxially stretched rubber. The network is trifunctional.

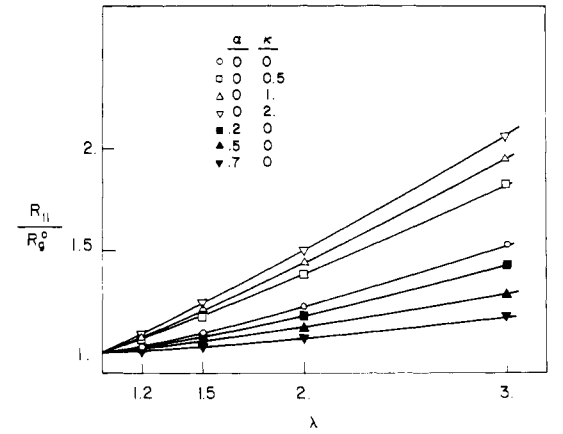

Figure 9. $R_{\parallel}/R_g^0$ vs. λ for a uniaxially stretched rubber. The network is tetrafunctional. The figure also applies to R_g/R_g^0 for a swollen rubber.

to that of the undeformed polymer chain. There are several generalities that hold for both the phantom and the real network. First of all, changes in molecular dimensions upon elongation are greater for networks of higher functionality. For example, in a phantom network stretched to twice its initial length, $R_{\parallel}/R_g^0$ takes on the values 1.22, 1.32, and 1.48 for $f = 3$, 4, and 10, respectively. Secondly, chain dimensions change relatively little in the direction perpendicular to stretch by comparison with changes parallel to stretch. For example, in a tetrafunctional phantom network stretched to three times its initial length, the polymer chains increase in size over 70%

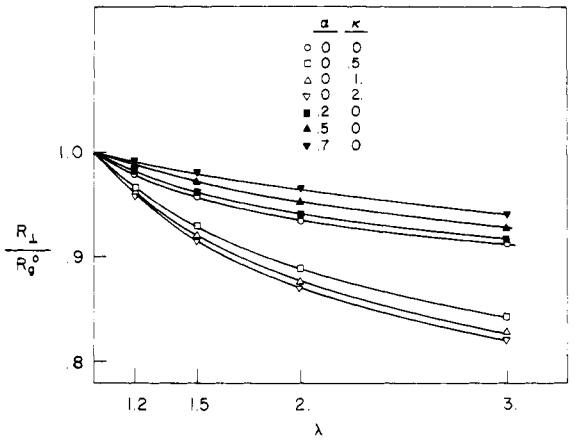

Figure 10. $R_\perp/R_g^0$ vs. λ for a uniaxially stretched rubber. The network is tetrafunctional.

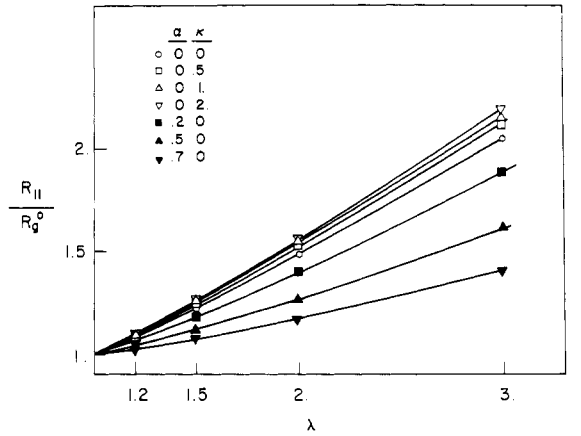

Figure 11. $R_\parallel/R_g^0$ vs. λ for a uniaxially stretched rubber. The network is decafunctional. The figure also applies to R_g/R_g^0 for a swollen rubber.

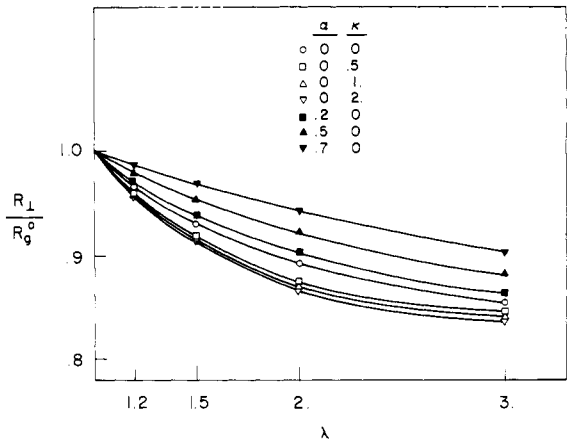

Figure 12. $R_\perp/R_g^0$ vs. λ for a uniaxially stretched rubber. The network is decafunctional.

measured in the parallel direction and decrease less than 9% in the perpendicular direction.

The insensitivity of scattering of networks of high functionality to changes in κ which can be seen in the scattering pattern (Figure 6) is evident in measurements of molecular radii. This is seen most clearly by comparing the results from trifunctional networks (Figures 7 and 8) with those of decafunctional networks (Figures 11 and 12). The tetrafunctional materials exhibit an intermediate behavior.

The plots of $S_\parallel(x)/S_D(x)$ vs. x in Figures 1, 3, 5, and 6 may be used for isotropic swollen networks because, as pointed out in the previous section, $S_\parallel(x)$ for a stretched chain and $S(x)$ for a swollen chain are given by the same formula. Also Figures 7, 9, and 11 for $R_\parallel^2$ of a stretched chain apply to R_g^2 of the swollen chain as well. This is based on the assumption that the swollen network is sufficiently concentrated that Gaussian chain statistics apply.[31] We emphasize once again that λ and λ* in the simply stretched networks refers to a different physical change than λ or λ* in the swollen network. It should not be expected that α and κ have similar values in these quite different experiments even if the same elastomer is used in the study.

Discussion

The equations developed and figures presented for this model of a real network are designed to provide a basis for comparison of SANS experiments on elastomeric networks with molecular deformation in these materials. A faithful comparison is not simple; in the model the chains are uniform in length, the functionality is known, cross-linking is complete, chains are linked at their ends, and there are no or very few dangling chain ends. Only one of the reported experiments seems to satisfy these criteria, that of Beltzung et al.[22] In our opinion, the preponderance of evidence supports the notion of network unfolding with limited chain extension in some cases, but further evidence is required to strengthen the case. The existence of this process, it should be noted, will have a profound influence on the classical models of rubber elasticity.

Having given this warning, it is particularly striking that the two experiments[18,19] (ref 19 has not yet appeared in the regular scientific literature) exhibit little chain deformation upon swelling. One important consideration in the swollen gel is that the polymer may take on many conformations prohibited in the bulk material by volume exclusion. Thus, in the presence of sufficient solvent, the polymer chains may reach an equilibrium in which a global rearrangement of cross-links can be achieved, corresponding to lesser stretching than would be found in a bulk material.

The model of reduced junction fluctuations proposed by Flory and adopted here contains the explicit assumption that the reduction in fluctuations is affine in the distortion of vectors connecting chain ends. This is a reasonable hypothesis, but it is not known whether it is correct.

The idea of network unfolding has been introduced without any attempt to relate the phenomenon to properties of the material. One can appreciate that increased entanglements would correspond to less unfolding, all other things being equal. As discussed above, the reduction in polymer concentration by swelling should lead to larger values of α than is seen in a stretching experiment with the same network. Also, preparation of networks in solution should reduce entanglements leading to lower κ and higher α.

While entanglements are involved in the present calculation to account for reduced junction fluctuations and to allow, by their absence, a type of network unfolding, they certainly play a direct role in reducing the available chain conformations. This direct role has not been incorporated in the present model. It could be described as a partial pinning of segments of a given chain by entanglements with other chains. An approximation to the direct effect of entanglements was given in ref 17, in which the entanglements were approximated by extra cross-links. The result was that chain distortion is enhanced by entanglemtns by comparison with the phantom network. Presumably the partial constraints induced by real entanglements would change the scattering law $S(\mathbf{q})$ in the same direction but to a lesser extent.

Network unfolding is described by a parameter α, but no theoretical construction has been provided to describe how α depends on network preparation, degree of network deformation, and quantity of solvent in the network. It merits a further analysis.

In summary, a set of calculations of scattering of labeled chains in polymer networks has been provided taking into account the restriction of junction fluctuations by entanglements and a rearrangement of parts of the network upon macroscopic deformation without stretching the polymer chains in the network. The SANS method provides a direct check on models of elastomeric deformation and constitutes an important and powerful method of critical evaluation of the theory and of estimating the significance of these modifications to the phantom model. The calculations are intended to serve as a basis for comparison with experimental studies on real networks.

Acknowledgment. The author is indebted to J. Bastide, R. Duplessix, and C. Picot for access to results of unpublished experiments and for interesting and illuminating related discussions. Generous support for this work was provided by the National Science Foundation under Grant DMR 79-262-54.

Appendix

The integral

$$I(x,y) = \int_0^1 (1 - w)e^{-xw-yw^2}\,dw \qquad \text{(A1)}$$

is needed for calculations of $S(\mathbf{q})$ of elastomeric networks. Typographical errors exist in an earlier publication,[17] and a corrected result is given here.

Case I: $y > 0$

$$I(x,y) = (\pi/4y)^{1/2} \exp[x^2/4y](1 + x/2y)[\text{erf}\,(y^{1/2} + x/2y^{1/2}) - \text{erf}\,(x/2y^{1/2})] - (1 - \exp(-x - y))/(2y) \qquad \text{(A2)}$$

Case II: $y < 0$, $y^* = -y$

$$I(x,y) = ((1 - x/2y^*)/y^{*1/2}) \exp[-(x - y^*)] \times [\text{Daw}\,(y^{*1/2} - x/(2y^{*1/2})) - \text{Daw}\,(x/(2y^{*1/2}))] + (1 - \exp[-(x - y^*)]/(2y^*)) \qquad \text{(A3)}$$

The error function, erf (x), is defined as

$$\text{erf}\,(x) = (2/\pi^{1/2}) \int_0^x e^{-y^2}\,dy \qquad \text{(A4)}$$

Dawson's integral is given by

$$\text{Daw}\,(x) = e^{-x^2} \int_0^x e^{y^2}\,dy \qquad \text{(A5)}$$

References and Notes

(1) James, H. M. *J. Chem. Phys.* **1947**, *15*, 651.
(2) James, H. M.; Guth, E. *J. Chem. Phys.* **1947**, *15*, 669.
(3) Graessley, W. W. *Macromolecules* **1975**, *8*, 186.
(4) Graessley, W. W. *Macromolecules* **1975**, *8*, 865.
(5) Ronca, G.; Allegra, G. *J. Chem. Phys.* **1975**, *63*, 4990.
(6) Deam, R. T.; Edwards, S. W. *Philos. Trans. R. Soc. London, Ser. A* **1976**, *280*, 1296.
(7) Flory, P. J. *Proc. R. Soc. London, Ser. A* **1976**, *351*, 351.
(8) Alfrey, T., Jr.; Lloyd, W. G. *J. Polym. Sci.* **1962**, *62*, 159.
(9) Lloyd, W. G.; Alfrey, T., Jr. *J. Polym. Sci.* **1962**, *62*, 301.
(10) Pearson, D. S.; Graessley, W. W. *Macromolecules* **1980**, *13*, 1001.
(11) Mark, J. E.; Sullivan, J. L. *J. Chem. Phys.* **1977**, *66*, 1006.
(12) Hvidt, S.; Kramer, O.; Batsberg, W.; Ferry, J. D. *Macromolecules* **1980**, *13*, 933.
(13) Cotton, J. P.; Decker, D.; Benoit, H.; Farnoux, B.; Higgins, J.; Jannink, G.; Ober, R.; Picot, C.; des Cloizeaux, J. *Macromolecules* **1974**, *7*, 863.
(14) Kirste, R. G.; Kruse, W. A.; Ibel, K. *Polymer* **1975**, *16*, 120.
(15) Pearson, D. S. *Macromolecules* **1977**, *10*, 696.
(16) Warner, M.; Edwards, S. F. *J. Phys. A* **1978**, *11*, 1649.
(17) Ullman, R. *J. Chem. Phys.* **1979**, *71*, 436.
(18) Benoit, H.; Decker, D.; Duplessix, R.; Picot, C.; Rempp, P.; Cotton, J. P.; Farnoux, B.; Jannink, G.; Ober, R. *J. Polym. Sci., Polym. Phys. Ed.* **1976**, *14*, 2119.
(19) Bastide, J.; Duplessix, R.; Picot, C. Franco-American Colloquium on Small Angle Scattering of X-Rays and Neutrons by Polymers, Strasbourg, Sept 16–19, 1980, lecture by C. Picot.
(20) Hinkley, J. A.; Han, C. C.; Moser, B.; Yu, H. *Macromolecules* **1978**, *11*, 836.
(21) Clough, S. B.; Maconnachie, A.; Allen, G. *Macromolecules* **1980**, *13*, 774. Agreement with the phantom network is fortuitous since the calculations were designed for end-linked chains and these networks were cross-linked by radiation.
(22) Beltzung, M.; Herz, J.; Picot, C.; Bastide, J.; Duplessix, R. "Abstracts of Communications of the 27th International Symposium on Macromolecules", Strasbourg, July 1981, Vol. 2, p 728.
(23) Han, C. C., private communication.
(24) Flory, P. J. *J. Chem. Phys.* **1977**, *66*, 5720.
(25) Erman, B.; Flory, P. J. *J. Chem. Phys.* **1978**, *68*, 5363.
(26) Gee, G.; Herbert, J. M. B.; Roberts, R. C. *Polymer* **1965**, *6*, 541.
(27) Yen, L. Y.; Eichinger, B. E. *J. Polym. Sci., Polym. Phys. Ed.* **1978**, *16*, 121.
(28) Flory, P. J. *Macromolecules* **1979**, *12*, 119.
(29) A related view of this problem has been put forth recently. See p 25 and Figure 3 of: Bastide, J.; Picot, C.; Candau, S. *J. Macromol. Sci., Phys.* **1981**, *B19*, 13.
(30) Debye, P. *J. Phys. Chem.* **1947**, *51*, 18.
(31) The calculation in a case where excluded volume effects are large has been done for the phantom network in ref 17. In this situation, $\langle r_{ij}^2 \rangle$ is a function of i, j, and n and not $|i - j|$ only. Accordingly, eq 5 does not hold.